SUPERCONDUCTIVITY – *Applied*

Evaluation of Adhesion Strength of Sol-Gel Ceramic Insulation for HTS Magnets

Celik, E., NHMFL and Sakarya Univ.-Turkey, Metallurgy
Hascicek, Y.S., NHMFL

Sol-gel is a very attractive low temperature processing technique for preparation of complex oxide compositions with high homogenity.[1] Coating failure is fundamentally related to the adhesion and cohesion strength. The aim of this study was to evaluate the adhesion properties of ceramic insulation on silver tapes as sheathing to HTS conductors.

The sols were prepared from MgO, Y_2O_3, SnO_2, and In_2O_3 doped Zr and Ce based precursor materials. The solutions were used for coatings on the silver tape by dipping at ambient atmosphere. The gel layers were transformed to amorphous layers at about 300 °C in 1 minute. The ceramic oxide coatings were heat treated at temperatures between 500 °C and 650 °C depending on the coating type. The lap joint samples were pulled to failure using a mini tensile tester.

The typical surface morphology of sol-gel coatings is shown in Figure 1. Although ZrO_2 and ZrO_2 based coatings exhibit the similar surface morphologies, which contain cracks, CeO_2 coating showed an almost crack-free surface. XRD results showed that sol-gel coatings started to crystallize at about 400 °C to 500 °C. Cubic, orthorhombic and tetragonal phases were clearly observed on the XRD patterns for ZrO_2 and ZrO_2 based coatings prepared from $Zr[O(CH_2)_3CH_3]_4$ precursor.

The main factor influencing adhesion properties is adhesive strength in coatings owing to a standard joint area. The adhesive strength (σ_s) is determined as the shear stress at which the joint abruptly yields. The value of adhesive strength of ZrO_2 joint was increased by doping with Y_2O_3, MgO, CeO_2, In_2O_3, and SnO_2. The best sample was ZrO_2+Y_2O_3 with σ_s=1.15 MPa (see Figure 2). The SEM observations of failure

surfaces strongly indicated that failure occurred at the interface of Ag substrates and coatings. In that case, the failure mode of thin films in the interface was mixed interfacial/cohesive defects.

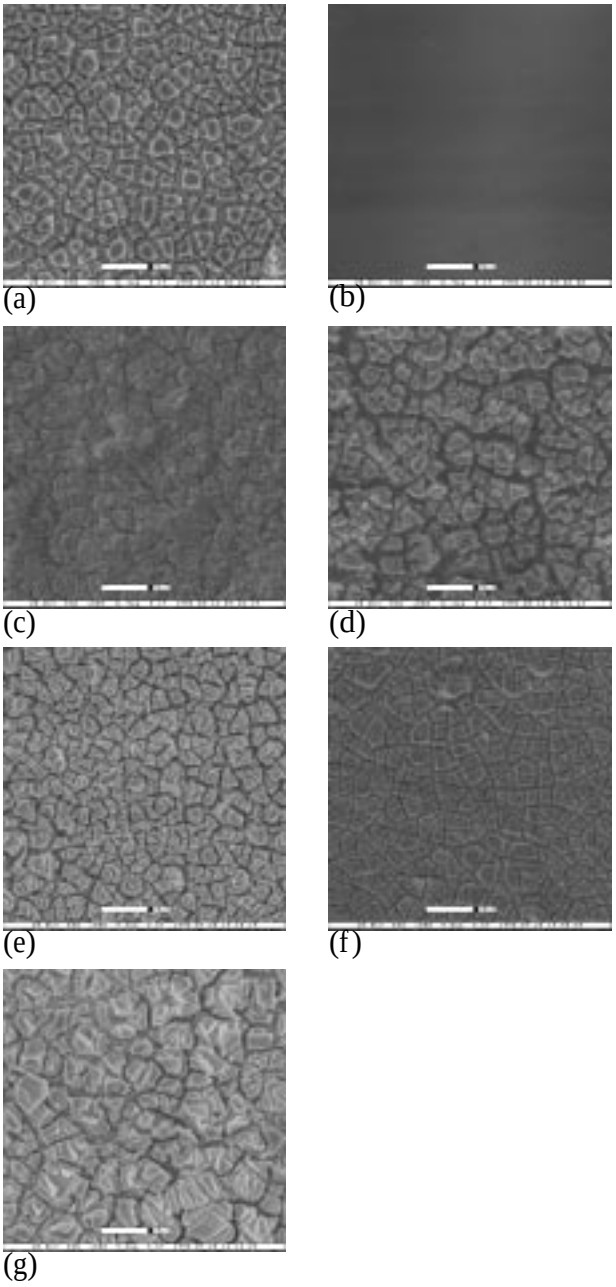

Figure 1. The surface topography of (a) ZrO_2, (b) CeO_2, (c) ZrO_2+MgO, (d) ZrO_2+Y_2O_3, (e) ZrO_2+CeO_2, (f) ZrO_2+SnO_2 and (g) ZrO_2+InO_2 coatings.

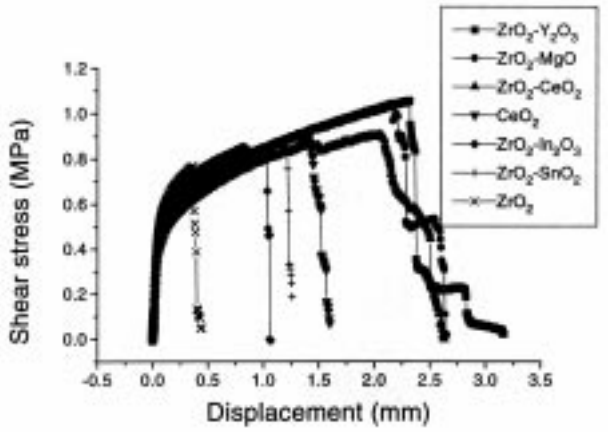

Figure 2. Shear stress vs. displacement for Ag substrates with joint made by ZrO_2+Y_2O_3, ZrO_2+MgO, ZrO_2+CeO_2, CeO_2, ZrO_2+SnO_2, ZrO_2+In_2O_3 and ZrO_2 coatings.

References:

1 Maleto, M.I., *et al.*, Thin Solid Films, 249, 1-5 (1994).

2 Brinker, C.J., *et al.*, Academic Press, Inc., ISBN: 0-12-134970-5, 839-881 (1990).

Sol-Gel Buffer Layers for YBCO: Growth and Processing

Celik, E., NHMFL and Sakarya Univ.-Turkey, Metallurgy

Hascicek, Y.S., NHMFL

Sol-gel CeO_2, yttria-stabilized zirconia (YSZ), MgO, $BaTiO_3$, $SrTiO_3$, $PbTiO_3$, $CdTiO_3$, $BaZrO_3$, $LaAlO_3$ thin films are used as buffer layers because they have several important advantages. These strengths include support-oriented growth of YBCO, oxidation protection of Ni for YBCO processing and orientation, and chemical compatibility on Ni.[1] The processing and growth mechanism of CeO_2 and YSZ buffer layers were evaluated on textured Ni substrates for surface coated YBCO conductor.

CeO_2 and YSZ buffer layers were prepared using solutions of Ce, Zr, and Y based organometallic compounds via non-vacuum sol-gel technique. The CeO_2 and YSZ were heat treated at temperatures of

500 °C and 600 °C, respectively. CeO_2 and YSZ formation starts at temperatures between 400 °C and 550 °C. Surface morphologies of CeO_2 and YSZ buffer layers are given in Figure 1.

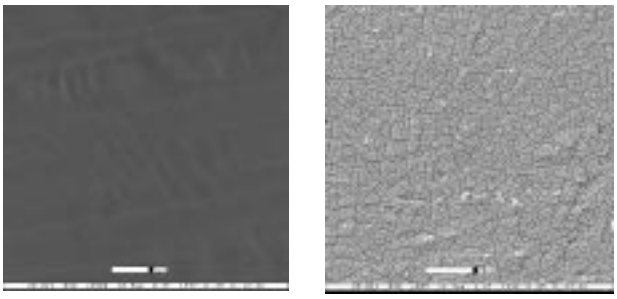

Figure 1. The surface topography of CeO_2 and YSZ thin films.

According to ESEM, DTA, and TGA studies, three main phenomena were determined from room temperature to oxide ceramic formation temperature; solvent removal, combustion of organic groups, and ceramic formation. Gel films at room temperature started to decompose at about 100 °C and 125 °C. Two endothermic reactions took place at temperatures of about 100 °C and 150 °C due to removal of solvent. The organic materials burned on surfaces at temperatures between 250 °C and 350 °C. All thin films showed that the sol-gel coatings remained in the amorphous state until 400 °C and 500 °C. With increasing heat treatment temperature to around 420 °C or higher temperatures, cubic CeO_2 and cubic YSZ thin films, with polycrystalline structure, were formed on the Ni substrate (see Figures 2 and 3). The layer thickness was found to be critical. For thicker CeO_2 and YSZ films on Ni substrates, crack formation was observed. One of the factors affecting the final thickness is amount of solvent in the sol. When the amount of precursor material increased in the solution, bubbles and microbubbles were produced on the surface. The bubbles started to cause the cracks on surfaces of gel films. The bubble formation changed according to the types of anions. The anions in solutions, solvent, and catalysts affected particle morphology, stability, and microstructure of thin films. Further research on buffer layers for surface coated YBCO conductors are necessary to understand interactions between solution preparation and film formation. After that, the textured Ni substrate will be coated with buffer layers for non-vacuum surface coated YBCO conductor development.

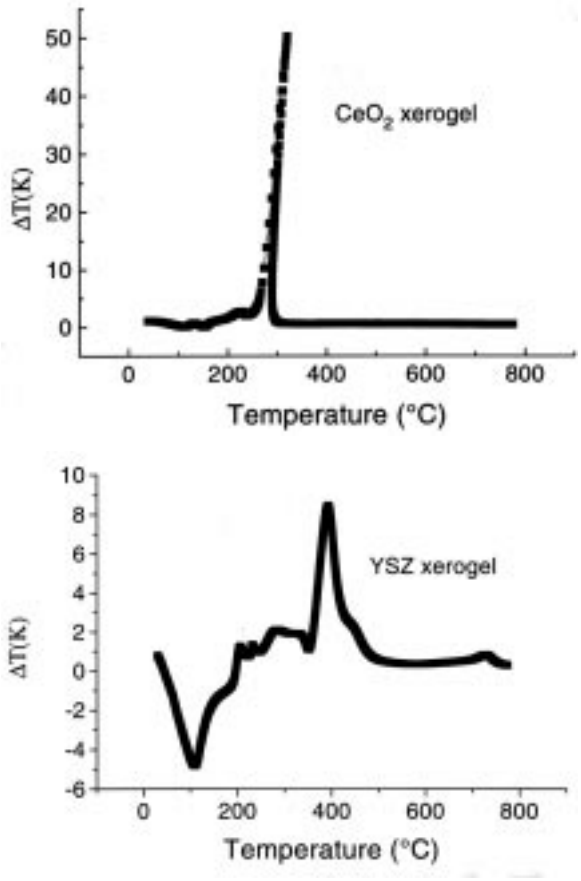

Figure 2. DTA curves of CeO_2 and YSZ xerogels.

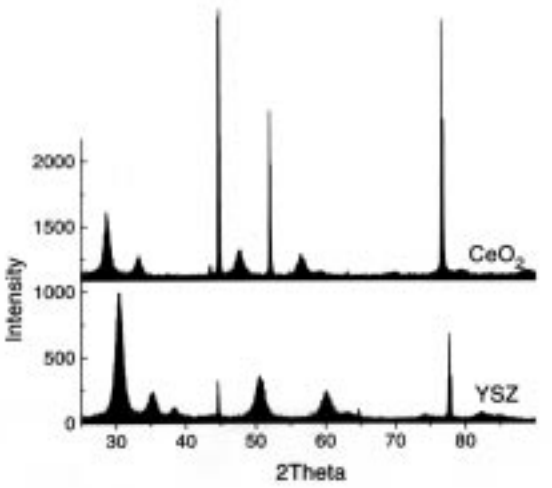

Figure 3. X-ray diffraction patterns of sol-gel CeO_2 and YSZ films.

Reference:

1 Tian, Y.J., *et al*., J. Superconductivity, 693-696, 7 (1994).

Critical Current of Superconducting Rutherford Cable Subjected to Transverse Pressure in High Magnetic Fields

Dietderich, D.R., Lawrence Berkeley National Laboratory (LBL)
Scanlan, R.M., LBL
Walsh, R.P., NHMFL
Miller, J.R., NHMFL

The large forces produced when superconducting magnets are energized can reduce the critical current of the conductor before the elastic limit is reached. To produce an optimum magnet design, which best utilizes the superconductor material, and maximizes the field the critical current variation with pressure, measurements are required. The magnets being designed and built in the Superconducting Magnet Group (SMG) of LBL require the flat superconducting cable of the magnet to be bi-axially stressed on both the face and the edge.

The results presented here are the first measurements performed at the NHMFL in a system designed for the SMG.[1] The NHMFL split pair solenoid magnet manufactured by Oxford Instruments can produce a field of 13 T, and can be oriented with the bore horizontal. A piston assembly designed for He gas pressures up to 10 MPa (1,500 psi) fits into the magnet bore, and can apply transverse specimen pressures of 380 MPa. This permits cables to be tested with the magnetic field perpendicular to the current in the cables. These tests were performed on two different cables designed for and used in the inner coils of the world record dipole magnet D20.[2] Two strands made by two manufacturers (TWC and IGC) were used in the Rutherford cables of this study (Figure 1). The TWC strand had more Cu stabilizer, and each of its 120 sub-elements had its own diffusion barrier. The IGC strand had less Cu stabilizer, and a diffusion barrier around all of its 19 sub-elements. The results for both cables showed that very little if any permanent degradation occurred for transverse loads from 185 MPa to 210 MPa. The critical current of the cable with IGC strand, however, was reduced by 40 % with a transverse pressure of 210 MPa at 11 T. The I_c of the cable with TWC strand was only reduced by 15 % at 11 T and 185 MPa.

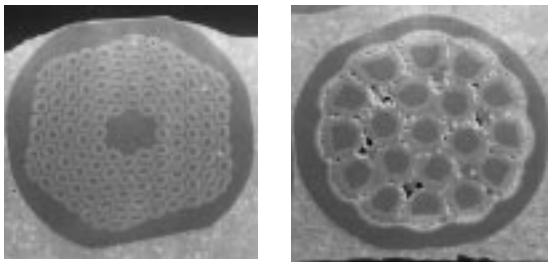

(a) (b)

Figure 1. (a) TWC strand of cable. (b) IGC strand of cable after heat treatment.

References:

1 Dietderich, D.R., *et.al.*, Proc. IEEE Trans. on Appl. Superconductivity, Sept 14-18, 1998, Palm Desert, CA.
2 McInturff, A.D., *et.al.*, Proc. Particle Accel. Conf., May 12-16, Vancouver, B.C. Canada.

n-Values for the Superconducting Transitions of Nb_3Sn Conductors for the Wide Bore 900 MHz NMR Magnet

Dixon, I.R., NHMFL
Markiewicz, W.D., NHMFL
Pickard, K.W., NHMFL
Swenson, C.A., NHMFL

Electrical characterization of the Nb_3Sn superconductor for application in the 900 MHz wide bore NMR magnet is performed. The magnet has five coils containing bronze process niobium-tin superconductor. Short samples of each of the five conductor types are reacted in a similar manner as the coils and the critical currents are measured.

The samples are mounted across a Ti-6Al-4V shunt, and the tests are conducted in background fields up to 19.45 T at temperatures of 4.2 K and 1.8 K. The measured current-voltage relationships of each conductor as expressed by the index number (n-value) are presented.

The construction of the superconductors is unique for each coil in dimensions and number of filaments. The superconductor designations and component fractions are listed in Table 1.

Table 1. Nb_3Sn superconductor component configuration.

Type	Coil	f_{Cu}	f_{SC}	$f_{Barrier}$
NSTT 86000A25	1	0.25	0.69	0.06
NSTT 62000A25	2	0.25	0.69	0.06
NSTT 64000A25	3	0.25	0.69	0.06
NSTT 62000A25	3	0.25	0.69	0.06
NST 39000A33	4	0.34	0.61	0.05
NST 28000A49	5	0.49	0.46	0.05

The n-value for each superconducting transition of the Nb_3Sn conductors was computed. The results are plotted in Figure 1 for measurements at 4.2 K and in Figure 2 for measurements at 1.8 K. The conductors for coils 1, 2, 4, and 5 all behaved similarly with respect to each other at 4.2 K, and the results are somewhat linear with field. Regarding coil 3 conductor, a greater amount of data was collected for type NSTT 64000A25 than NSTT 62000A25. In contrast to the critical current, conductor type NSTT 62000A25 has n-values approximately 20% higher than type NSTT

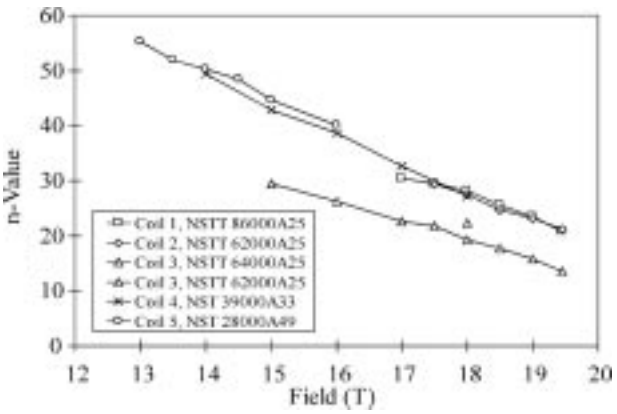

Figure 1. n-Values of conductors from each coil of the 900 MHz NMR magnet as a function of field and at 4.2 K.

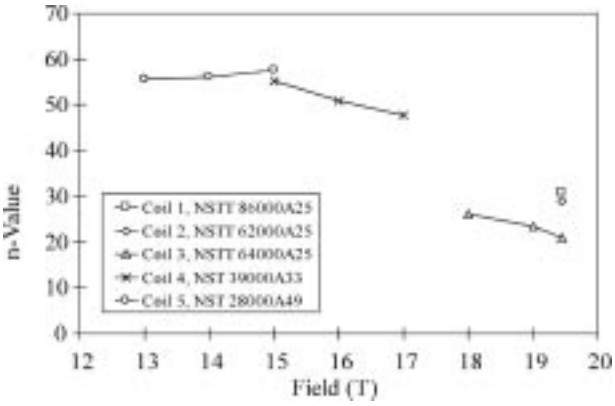

Figure 2. n-Values of conductors from each coil of the 900 MHz NMR magnet as a function of field and at 1.8 K.

64000A25. The effects of the lower n-value of conductor type NSTT 64000A25 is somewhat offset by its relatively high critical currents.

EURUS HTS Current Lead Development for 45 K Operation

Hascicek, Y.S., NHMFL
Hodges, R., EURUS Technologies
Eyssa, Y., NHMFL

An HTS current lead in the shape of the letter J (referred as the J-bar in the text) is needed for 45 K operation in the background field of about 0.2 T. Bi-2223/Ag multifilamentary tape conductor was used in the fabrication of the J-bar.

The critical current density (I_c) versus temperature profile between 4.2 K and T_c of the conductor was measured. The critical current at 77 K and 45 K were found to be 23 A and 80 A, respectively, both at zero applied field. In addition, I_c (at 4.2 K) of several samples taken from different parts of the conductor was measured to verify that I_c was uniform along the length of the conductor. It was found that I_c at 4.2 K was 170 A with a 5.8% variation.

A piece of conductor was always exposed to each step of the fabrication process before the step was adopted. The I_c of that piece was measured at 4.2

K. The variation in I_c was well within the measured 5.8% variation along the length.

Special heating strips were used to heat the channels after the HTS tapes were stacked in. Three kinds of solder, with three different melting temperatures, were used to solder the tapes in the channels.

Each channel has two stacks, each of which has 33 of these tapes, and the J-bar consists of four channels (as seen in Figure 1). Therefore the J-bar has 4 x 2 x 33 = 264 tapes.

Figure 1. One J-bar as finished. The overall length of the J-bar is 0.6 m.

The self field of the J-bar was modeled, and it was found to be 0.044 T, and tangential to the surface. We took the worst case scenario and assumed 0.16 T background field (The specs called for 0.12 T during operation.). Therefore, I_c of the J-bar at 45 K and 0.16 T, by using the profiles in Figure 2, is expected to be 2.75 x 23 A x 264 = 16698 A .

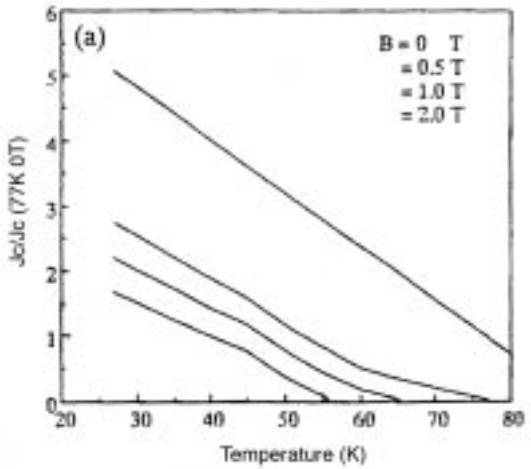

Figure 2. (Ic)/{Ic(77 k, 0 T)} vs. temperature profiles at 0 T, 0.5 T, 1.0 T, and 2.0 T for J normal to B and B normal to the tape surface.

The I_c of the J-bar at 45 K and zero applied field is expected to be 264 x 80 A = 21120 A (no self field correction is taken into account here.).

The I_c of the J-bar at 45 K and 0.54 T (0.5 T applied and 0.04 T self field maximum expected fault condition) is expected to be 1.5 x 23 A x 264 = 8486 A. The critical current of the J-bar will be measured at 77 K before installation.

This project was supported by EURUS Technologies.

High Field Characterization of Novel Nb_3Sn Tape Conductors

Hascicek, Y.S., NHMFL

A novel processing technique was developed to fabricate $(Nb, Ta)_3Sn$ tape conductors by Professor Tachikawa of Tokai University, Japan. This tape conductors showed critical current densities above 23 T when measured at Japan. I have measured the critical current density of these tape conductors in the 30 T resistive magnet up to 27 T applied fields at NHMFL. To my knowledge this is the first Nb_3Sn conductor that remained superconducting, and carried practical current (I_c was 80 A at 22 T, and 20 A at 25 T) up to 26 T.

This new development in the Nb_3Sn could open up the way for fabricating 1 GHz NMR using LTS conductors only.

Recent Developments of Bronze Processed Nb_3Sn Superconducting Wire at Oxford Instruments, Inc., Superconducting Technology (OI-ST)

Hentges, R., Oxford Instruments, Inc., Superconducting Technology (OI-ST)
Zhang, Y., OI-ST
Hong, S., OI-ST

Oxford Instruments, Inc., Superconducting Technology (OI-ST) has been continuously improving the high field performance of bronze processed Nb_3Sn wires for NMR use. It is well known that doping Nb_3Sn with either titanium or tantalum increases the upper critical field.[1,2] OI-ST has recently developed internally stabilized wire using bronze that was doped with titanium. The filaments were doped with tantalum. Similar wires, without the titanium additions to the bronze, were made for comparison. These wires were tested at NHMFL using a 20 T resistive magnet. Critical current was measured at 4.2 K and 2.2 K using a criterion of 0.1 uv/cm with the wire fully soldered to a stainless steel test barrel.

The extrapolated upper critical field at 4.2 K of the $(NbTa)_3Sn$ wire was 24.6 T. The wire with titanium doping had an extrapolated B_{c2} of 26.6 T. At 18 T, the enhancement in current density due to the titanium doping was nearly 20 %. With the heat treatment that was employed, the titanium doped wire had lower current than the $(NbTa)_3Sn$ wire at fields below 15 T. The figure shows relative current density of the two wires as a function of magnetic field along with the percent difference.

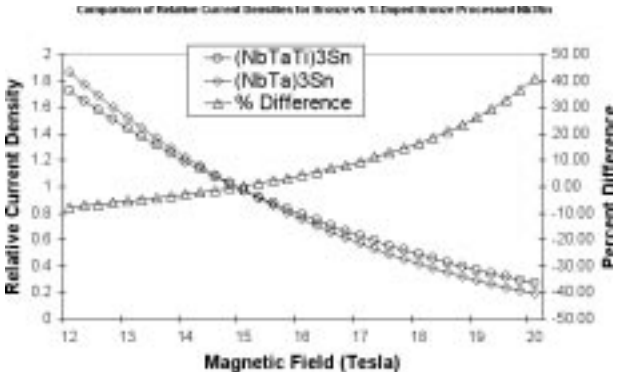

Figure 1. Relative current density vs. magnetic field.

References:

1 Miyatake, T., *et al*., Proc. of the 9th US-Japan Workshop on High Field Superconductors, 995 (1995).
2 Krauth, H., *et al*., High Magnetic Fields, 403 (1997).

Heat Treatment of Pulsed Laser Deposited YBCO Thin Films in Magnetic Fields Up to 20 T

Hodges, R.G.L., EURUS Technologies
Kugeler, O.J., NHMFL/RWTH-Aachen
Muenchausen, R.E., EURUS Technologies
Durbin, S.M., FAMU-FSU College of Engineering
Hascicek, Y.S., NHMFL
Schwartz, J., NHMFL

Materials that have an anisotropic magnetic susceptibility close to their melting temperature can be textured by heat treatment in a magnetic field, as grains tend to align with their easy axis of magnetization parallel to the field direction. Even at these elevated temperatures, however, this movement can be suppressed by limited grain boundary mobility.

Studies are been undertaken to investigate if this effect is strong enough to be of large scale practical use in the texturing of thin films of YBCO at temperatures significantly below the peritectic temperature (Tp). Pulsed laser deposited amorphous YBCO thin-films on lanthanum aluminate substrates were post annealed in a furnace, purposely designed and built as an inset for the 20 T, 200 mm bore resistive magnet.

Presently, the processing parameters that have been investigated include: annealing temperature, (700

°C, 750 °C, and 800 °C); magnetic field strength (19 T, 17 T, and 0 T); the orientation of the film surface with respect to the magnetic field lines (parallel and perpendicular); and heat treatment time (2 hrs., 3 hrs., and 4 hrs.). All of the above parameters were varied while the processing pressure was maintained at atmospheric pressure.

Under the conditions described above, any influence of magnetic field upon the re-crystallization behavior of these thin films appears to be very small. This is evidenced by Figure 1 where there appear to be no clear differences between XRD traces for samples processed in magnetic field, with different orientations, and out of magnetic field.

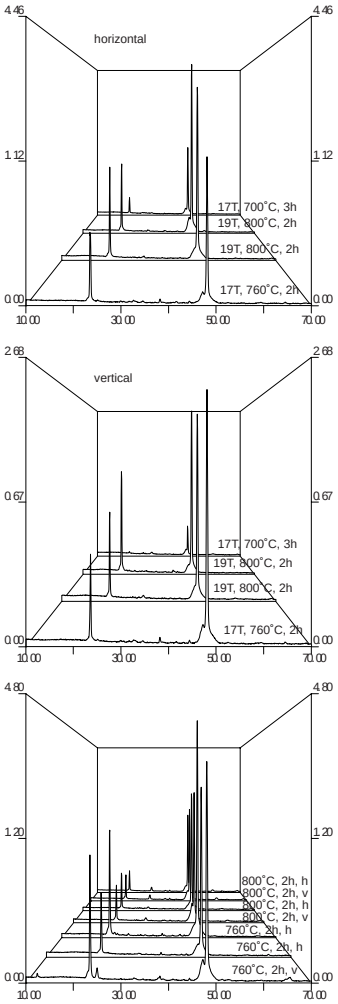

Figure 1. XRD traces for YBCO thin films heat treated under different conditions of temperature, time and magnetic field, in horizontal and vertical orientations (a and b), and different temperature and time in the absence of a magnetic field (c).

In the future, we intend to reduce the processing pressure at which these samples are heat treated. Reducing the pressure has the effect of lowering Tp, which should increase grain boundary mobility for a particular processing temperature, and aid in the formation of the final desired texture within the material.

Continuous Processing of $Bi_2Sr_2CaCu_2O_8$ Tapes

Hu, Q.Y., NHMFL
Schwartz, J., NHMFL and FAMU-FSU College of Engineering

The Ag-sheathed Bi2212 tape has high J_c and is easy to fabricate because a partial melting process can be applied. The partial melting process increases the mass density of the core, and improves the connectivity and the alignment of the Bi2212 grains. For large size coils, however, the melting process is very difficult to apply, because their thermal mass makes controlling melting time difficult. The fabrication of Ag-sheathed Bi2212 coil using a react-wind-sinter technique (R-W-S) is advantageous over the wind-and-react or react-and-wind techniques in terms of reducing handling damages, and achieving high critical current density over a long length. In this technique, long lengths of the Ag-sheathed Bi2212 tape are reacted uniformly by pulling the tape continuously through a precisely defined temperature profile. Our previous work[1] has investigated the feasibility of the R-W-S process being applied to the Ag-sheathed Bi2212 tape, mainly on monofilamentary tapes. In our recent work, we applied R-W-S process to the high alloy AgMg-sheathed Bi2212 multifilamentary tape. Here we call it continuous processing.

The multifilamentary Bi2212 tape was fabricated by the well-established powder-in-tube technique. The commercial powder of nominal stoichiometric composition of $Bi_{2.1}Sr_{1.7}Ca_{1.2}Cu_{2.0}O_x$ was used as the precursor. The sheathed material is pure Ag for the inner tube, and Ag alloy for the outer tube containing 1.2 at% Mg. After the drawing and rolling process, the final tape dimensions are 3 mm

in width and 0.22 mm in thickness. The continuous processing was carried out in a quartz furnace, which consists of three hot zones: (1) a homogeneous zone as long as 263 mm located in the middle of the furnace with a temperature variation of <±1 °C, (2) a homogeneous zone as long as 585 mm located in the middle of the furnace with a temperature variation of <±3 °C, and (3) two zones with a gradient of about 3 °C/cm. From those configurations, the peak temperature is 866±3 °C.

From Figure 1, it is seen that with increasing pulling speed, the I_c of the continuous processed samples increases until reaching 16.6 mm/min, or 1 m/h. This result is encouraging from the point of view of reducing processing time.

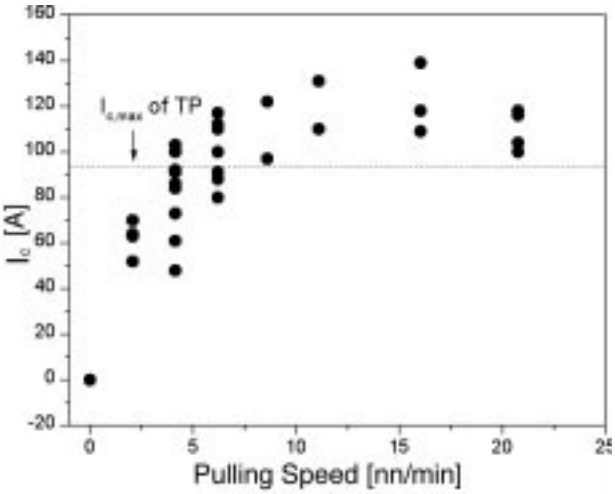

Figure 1. I_c vs. sample pulling speeds in continuous processing.

For traditional processing, the temperature along the tape length is uniform. For continuous processing, however, the temperature of a tape is different from point to point at the same time when it is in the gradient zones, which is the feature of directional solidification. Directional solidification is a method to prepare materials of a preferred grain orientation parallel to the sample axis, along which the temperature gradient applies. Bi2212 phase forms in peritectic reaction,[2,3] Bi2201 + $(Sr,Ca)CuO_2$ + L → Bi2212. According to our DTA data, the re-crystallization temperature of Bi2212 phase is around 860 °C. From the melting temperature down to 860 °C, as the temperature decreases, the content of the Bi2201 phase in the liquid increases. We propose that in the cooling zone, a small number of Bi2201 can grow to large size by directional solidification, instead of more grains forming. In the subsequent cooling process around 860 °C, the large Bi2201 grains are beneficial to the formation of aligned Bi2212 grains since they can serve as matrixes for Bi2212 grains to grow on epitaxially. Also, around 860 °C, the Bi2212 can directly nucleate from the liquid,[2] and with the help of the directional solidification, grow to large aligned grains. In continuous processing, for those Bi2212 grains whose basal planes are parallel to the temperature gradient direction, their ab-planes would grow even faster than in traditional processing. The misalignment of grains, therefore, is further reduced or the grain alignment is enhanced (Figure 2), which results in increased J_c.

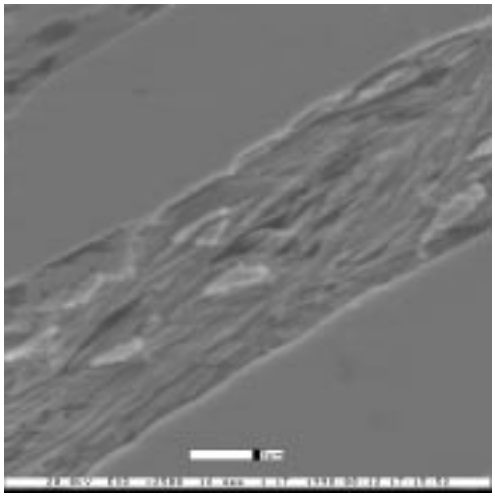

Figure 2. ESEM micrographs of the samples of continuous processing.

References:

1 Boutemy, S., *et al.*, IEEE Trans. Appl. Supercond., 1553, 7 (1997).
2 Hellstrom, E.E., High Temperature Superconducting Materials Science and Engineering, 383-439, (1994).
3 Suzuki, T., *et al.*, Physica C, 173, 301 (1998).

Heat Treatment of Conductors and Coils for 3 T Insert Coils

Hu, Q.Y., NHMFL
Hascicek, Y., NHMFL
Schwartz, J., NHMFL/FAMU-FSU College of Engineering

Our recent efforts to build a 3 T HTS insert coil for the 1.1 GHz NMR demands high quality Bi2212 pancakes. There are two kinds of sheath for the conductors used for the coil; pure Ag and AgMg alloy. The program used for heat treatment consists of four stages: pre-annealing, partial melting, slow cooling, and post-annealing. The pre-annealing process enables contaminate carbon to react with oxygen (forming CO_2) and diffuse out of the sheath, which is especially important to long tapes. The partial melting process enhances mass transport, and prepares the liquid phase for subsequent re-crystallization. The slow cooling enables the formation of well-aligned large Bi2212 grains. The post-annealing further aligns the grains.

Our experiments indicated that among all heat treatment stages, the melting process is the most important. Our efforts, therefore, concentrated on the optimization of the melting temperature to obtain the highest I_c. Figure 1 shows the results of the I_c of the AgMg sheathed Bi2212 tape melted at different temperatures. It is seen that the I_c is almost zero below a critical temperature (T^c_1, around 885 °C), increases quickly as T^c_1, reaches

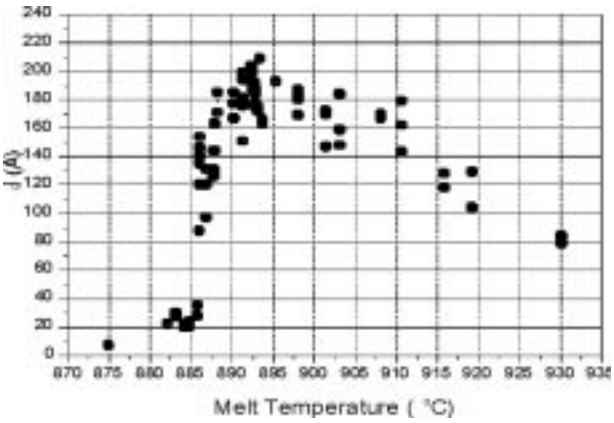

Figure 1. Program used for tape heat treatment.

the maximum at T^c_2 (893 °C), and finally drops slowly above T^c_2. The pure Ag sheath has the same behavior (Figure 2).

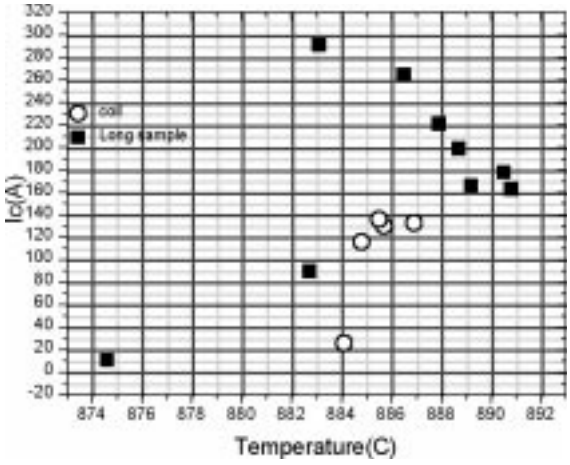

Figure 2. Critical current vs. melting temperature.

The DTA measurements show that the melting temperature of the tape is 883 °C. The highest I_c, however, is obtained at a higher temperature, 893 °C (T^c_2). This is understandable because higher temperature melting is beneficial to atom diffusion due to lower viscosity of the melt. Furthermore, the thermocouples in different devices have different calibrations. The reason why I_c drops above T^c_2 is probably because an over-melting leads to formation of large 1:1 AEC grains,[1] which hardly decomposes in the following heat-treatment. Also, the melt flows out of the Ag sheath more easily from the pinholes at high temperatures due to the lower viscosity, which is a common deformation defects in the PIT tapes. This also degrades the phase purity of the tape due to the overall composition of the filaments being off stoichiometry of Bi2212.

The XRD results demonstrate that with gradual increasing of the peak temperature, the impurity content decreases at first, and subsequently increases again above T^c_2. Without melting, the sample contains large amounts of second phases, the grains are not well connected, and the alignment is poor. After melting, all these are improved and the tape appears.

Although the melting point of Ag drops quickly, with the addition of Mg, according to the phase diagram,

our DTA measurements showed that the AgMg and Ag sheath had the same melting point (935 °C) in an O_2 atmosphere. This may be because Mg oxidizes at low temperatures, which does not influence the melting behavior of Ag at high temperatures. Recently, we have achieved a high I_c with AgMg-sheathed tapes (305 A) with a J_c of >200 kA/cm² at 4.2 K and self-field. The maximum I_c with pure Ag sheath is 410 A. Since the I_c drops slowly with temperatures over T^c_2 when we heat treated a coil, we chose a temperature of one or two degrees higher to ensure a real melting (Figure 2).

Reference:

1 Hellstrom, E.E., High Temperature Superconducting Materials Science and Engineering, 383-439 (1994).

Recent Progress on the Usage of Sintering Aids to Improve the Texture in $YBa_2Cu_3O_{7-\delta}$ Coatings

Kugeler, O., NHMFL/RWTH Aachen, Germany
Sahm, P.R., RWTH-Aachen, Germany
Schwartz, J., NHMFL
Hascicek, Y.S., NHMFL

The degree of texture and weak-links between adjacent grains are the main factors influencing high critical current densities in YBCO-films. For large scale, low-cost production of tapes it is desirable to produce the material with a technique that works under a non-vacuum atmosphere.

We investigated the influence of a sintering aid, tin(IV)iodide, on the thermal behavior of YBCO coatings during heat treatment. Prior to heat treatment the YBCO powder was stirred in a solution of tin(IV)iodide in acetone that yielded a thin coating of tin(IV)iodide on the surface of the powder particles after evaporation of the acetone.

Tin (IV)iodide undergoes a surface reaction with YBCO, which can be seen from thermogravimetric analysis (TGA) (Figure 1), and differential thermal analysis (DTA) (Figure 2). TGA has been done with three different powders. The first curve shows pure YBCO powder that suffers a weight loss mainly due to oxygen loss from the orthorhombic to tetragonal transition at about 550 °C. The coated powder suffers a weight loss at about 364 °C from evaporation of tin(IV)iodide. Yet not all of the tin(IV)iodide escapes. A part of it must have undergone a surface reaction with the YBCO phase. This is confirmed by the TGA of a coated powder pretreated at 400 °C for 12 hours, which is missing the evaporation of unreacted SnI_4, but shows the same increased weight loss at higher temperatures. DTA investigations of powders with different weight ratio YBCO/SnI_4 suggest that the

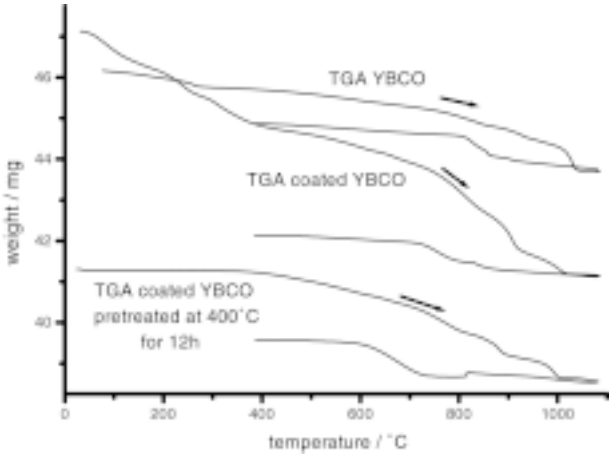

Figure 1. Thermogravimetric analysis of YBCO, tin(IV)iodide coated YBCO and a pretreated coated YBCO powder.

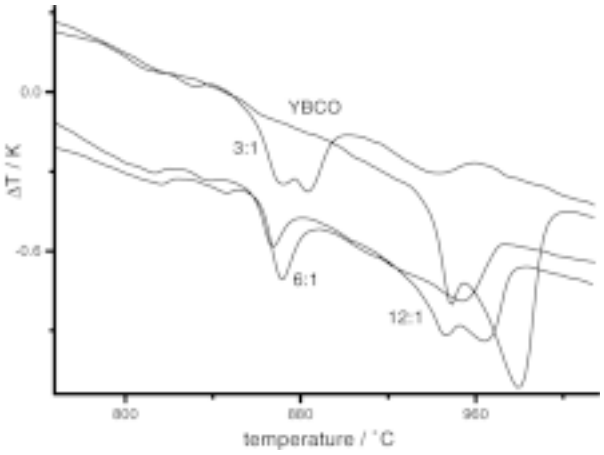

Figure 2. Differential thermal analysis investigations of SnI_4 coated YBCO powders. With increasing SnI_4 content an additional melting peak occurs below the peritectic melting temperature of YBCO.

presence of SnI_4 causes an additional melting peak at lower temperatures. The existence of a melting peak at lower temperatures could reduce the processing temperatures of YBCO and make processing on technical substrates like silver or silver-palladium feasible.

YBCO tapes will be fabricated from SnI_4 coated powders on CeO_2-buffered Nickel substrates and also on Ag, Ag-Pd substrates.

Influence of Silver and Gold Interfaces on the Formation and Stability of HgX1212 and HgX1223 Superconductors (X=Re, Pb, and Bi)

NHMFL

Roney, A.B., NHMFL/FAMU-FSU College of Engineering
Schwartz, J., NHMFL/FAMU-FSU College of Engineering
Sastry, P.V.P.S.S., NHMFL

A necessary step in the large-scale application of HgX1223 and HgX1212 superconductors is the development of metal-clad conductors. Toward that end, an important step is to understand the effect of metallic interfaces on the formation and stability of HgX1212 and HgX1223 superconductors. Fabrication of metal-clad conductors of Hg-superconductors is complicated due to the formation of amalgams that melt at much lower temperatures than the corresponding metals. As a first step in understanding the role of silver and gold interfaces on the formation of HgX1212 and HgX1223 superconductors, thick coatings of BaCaCuO precursors were applied on silver and gold foils, which were reacted using $CaHgO_2$ as the external Hg source in sealed quartz tubes. The reaction temperature was varied from 700 °C to 850 °C. It was observed that HgPb1223 and HgPb1212 could be synthesized on silver foil in the narrow temperature range of 760 °C to 780 °C. Silver foils melted at temperatures higher than 780 °C due to amalgamation. The microstructural characteristics of HgPb1223, formed on silver at 780 °C, were superior to that of the corresponding bulk samples in terms of both grain size and texture (Figure 1). Similar observations were made on HgBi1223 synthesized on gold foils.[1] Detailed investigations on the role of silver in controlling the Hg pressure at the oxide interface, and its effect on the microstructure of HgX1223 superconductor are in progress.

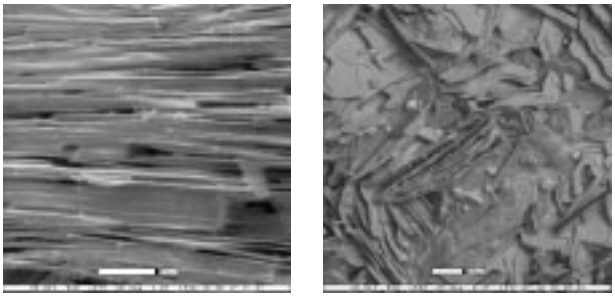

Figure 1. Microstructures of HgPb1223 synthesized on Ag foil and in bulk.

Studies are also being conducted to understand the role of temperature in the absorption of silver. These studies are aimed at utilizing the temperature dependent solubility of Hg in silver to release Hg from Ag-Hg for the conversion of BaCaCuO precursors into HgX1212 and HgX1223 superconductors in a powder-in-tube configuration. A significant amount of Hg was successfully loaded into Ag tubes at room temperature. These Hg-loaded Ag tubes were filled with BaCaCuO precursor powders, and deformed into wires and tapes. Investigations on the optimization of heat treatment conditions for HgX1223 formation are in progress.

Reference:

1 Amm, K.M., *et al.*, Superconductor Science and Technology, 11, 793 (1998).

Development of High Performance NbTi Superconductors

Rudziak, M., Supercon Inc.
Wong, T., Supercon Inc.
Frost, D., Supercon Inc.

Supercon Inc. has continued to develop NbTi superconductors for high field use by focusing on performance levels greater than 9 T. In order to improve the high field performance, Nb pins were added to the NbTi matrix, reducing the overall composition from Nb47wt%Ti to Nb44wt%Ti. According to current mixing theory, the ~4vol% Nb pins improve the H_{c2} of the alloy by reducing the Ti percentage of the alloy to the peak H_{c2} value when the average size of the Nb pins is reduced to less then the coherence length. This composite should not suffer from the H_{c2} suppression that is commonly seen with other artificial pining center materials.

The Nb/NbTi composite is also processed like a conventional NbTi superconductor, including precipitation heat treatments to form alpha titanium pinning sites. The heat treat temperatures are low enough not to cause diffusion of the Nb into the alloy matrix. The Nb pins are thus additive to the Ti pins, increasing overall pinning volume fraction. NHMFL facilities were used to test critical current, critical temperature, and upper critical fields at temperatures of 4.2 K and 1.8 K, at fields from 9 T to 12 T of samples produced by this process.

Synthesis, Phase Stability, and Properties of Hg-X-Ba-Ca-Cu-O Superconductors (X = Bi, Pb, and Re)

Sastry, P.V.P.S.S., NHMFL
Li, Y., NHMFL/FAMU-FSU College of Engineering
Peterson, S.C., NHMFL/FAMU-FSU College of Engineering
Schwartz, J., NHMFL/FAMU-FSU College of Engineering

A systematic study was conducted to understand the sequence of reactions that occurs during the synthesis of $(Hg,X)Ba_2Ca_2Cu_3O_y$, X = Re, Bi and Pb (Hg1223). The formation and decomposition of the intermediate phases during the high temperature reaction were followed as a function of temperature. HgX1223 phase forms over a wide range of temperatures, 750 °C to 950 °C, 750 °C to 880 °C, and 840 °C to 880 °C, for X = Re, Pb and Bi, respectively. At T < 750 °C, HgA1212 phase forms for X = Re and Pb.

Figure 1 depicts the stability windows for all three dopants studied.[1] Figure 2 depicts the stability of HgRe1201, HgRe1212, and HgRe1223 phases as a function of starting composition. The studies showed that control of the reaction temperature is crucial for

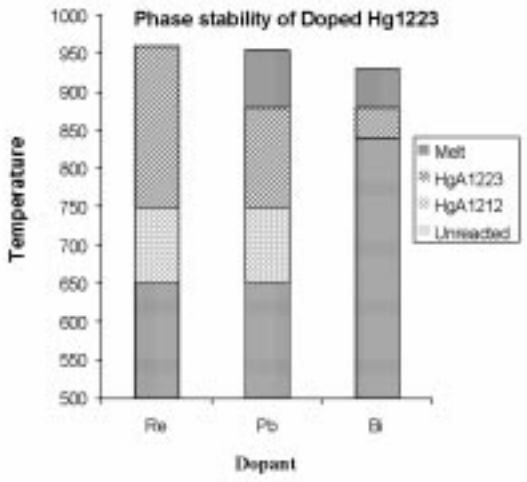

Figure 1. Phase stability of HgX1223 for x=Re, Pb, and Bi.

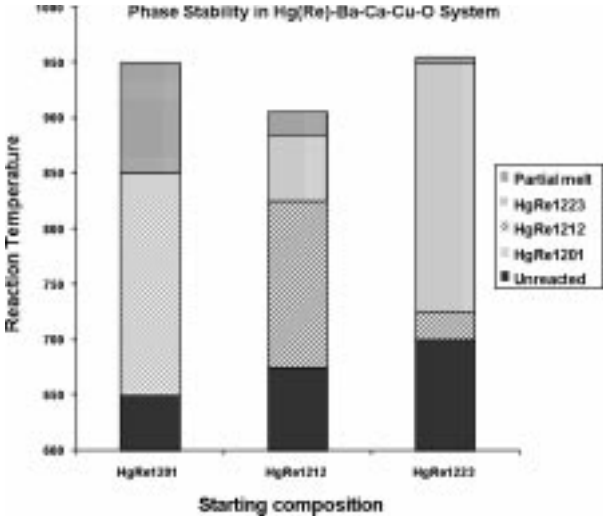

Figure 2. Phase stability of compositions Hg(Re)-Ba-Ca-Cu-O compositions.

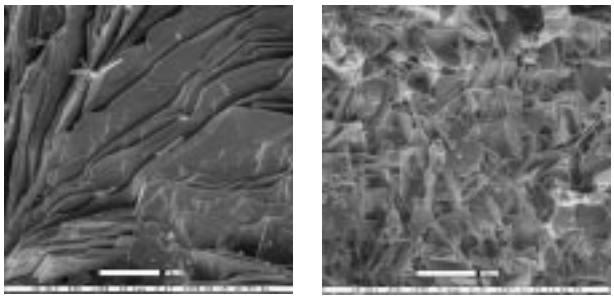

HgRe1212 HgRe1223

Figure 3. Typical microstructures of HgRe1212 and HgRe1223 materials.

achieving high phase purity in HgRe1212 and HgRe1223 phases.[2] The melting characteristics, and hence the microstructure of the final product, depend on the starting composition. Figure 3 shows the microstructures of HgRe1212 and HgRe1223 phases synthesized. Heat treatment conditions were optimized for the synthesis of pure HgX1212 and HgX1223 materials using commercial BaCaCuO precursor powders. Control of the Hg pressure during the reaction is crucial for achieving phase purity, grain growth, and texture in the final products.[1-4]

References:

1 Sastry, P.V.P.S.S., *et al.*, J. Superconductivity, 595, 11(1998).
2 Sastry, P.V.P.S.S., *et al.*, IEEE Transactions on Applied Superconductivity, in press.
3 Sastry, P.V.P.S.S., *et al.*, Physica C, 223, 297 (1998).
4 Sastry, P.V.P.S.S., *et al.*, Physica C, 125, 300 (1998).

Persistent Joint Development for High Field NMR

Swenson, C.A., NHMFL
Markiewicz, W.D., NHMFL

The persistence requirements of NMR impose limits on the total magnet circuit resistance. Resistance is determined by the field integrated resistive *n*-value loss in the coils, and the resistive sum from the joints. An NMR magnet requires several joint configurations to allow fabrication and assembly of the circuit. There are joints between Nb_3Sn conductors inside coils, NbTi conductors, and persistent joints between NbTi and Nb_3Sn conductors. A range of processing method is required given the complexity of the assembly.

Persistent joints were studied using a four-wire resistance measurement technique to compare joint performance. Resistance measurements were bipolar and at 500 A. Measurements were made at 4.2 K in liquid helium. Two methods of NbTi-NbTi joint fabrication have been evaluated: the diffusion bonding method, and a solder matrix replacement method using PbBi eutectic solder.

The diffusion bonding method has been shown to perform reliably at fields up to 2 T. The diffusion bonding process works with both bare NbTi and Nb coated multifilamentary conductors. The process has also been shown to be compatible with processing in a flowing argon environment. Table 1 presents a measurement summary for the diffusion bonded joints.

The PbBi eutectic alloy has been used as a superconducting solder to make a persistent joint. The joints were fabricated using a solder matrix replacement method to remove the copper from a multifilamentary NbTi wire. The NbTi-NbTi joints performed reliably at fields up to 1.5 T with the PbBi eutectic solder alloy. Table 2 presents a summary of the measurements using the PbBi solder.

The solder matrix replacement method has been extended to manufacture persistent joints with bronze process Nb_3Sn conductor.

The solder matrix replacement produced NbTi-Nb_3Sn persistent joints that perform in the 1 T range. Table 3 presents a summary of the measurement data.

Table 1. Diffusion bonded joint measurements.

Sample	R [Ω] B=0.5 T	R [Ω] B=1.0 T	R [Ω] B=2.0 T	R [Ω] B=3.0 T
A	$<1x10^{-11}$	$<1x10^{-11}$	$<1x10^{-11}$	
B		$<1x10^{-11}$	$<1x10^{-11}$	
C		$<1x10^{-11}$	$<1x10^{-11}$	
L	$<1x10^{-11}$	$<1x10^{-11}$	$<1x10^{-11}$	
M			$<1x10^{-11}$	
N			$<1x10^{-11}$	
R	$<1x10^{-11}$		$<1x10^{-11}$	$1.5x10^{-11}$
S	$<1x10^{-11}$	$<1x10^{-11}$	$<1x10^{-11}$	$1x10^{-11}$
T		$<1x10^{-11}$	$<1x10^{-11}$	$1.5x10^{-9}$

Table 2. Measurements on PbBi solder joints.

Sample	Solder	R [Ω] B=0.5 T	R [Ω] B=1.0 T	R [Ω] B=1.5 T
A	PbBi	$<1x10^{-11}$	$<1x10^{-11}$	$<1x10^{-11}$
B	PbBi	$<1x10^{-11}$	$<1x10^{-11}$	$<1x10^{-11}$
C	PbBi		$<1x10^{-11}$	$<1x10^{-11}$
D	PbBi		$<1x10^{-11}$	$<1x10^{-11}$
E	PbBi		$<1x10^{-11}$	$<1x10^{-11}$
F	PbBiSn	$6x10^{-11}$		$7x10^{-9}$
G	PbBiSn		$<1x10^{-11}$	$2x10^{-9}$
H	PbBiSn		$<1x10^{-11}$	$6x10^{-10}$

Table 3. Measurements on Nb_3Sn–NbTi joints.

Sample	Process	R [Ω] B=0.5 T	R [Ω] B=1.0 T	R [Ω] B=1.25 T
C	PbBi	R		
D	PbBi	$2x10^{-10}$		
E	PbBi		$<1x10^{-11}$	R
F	PbBi		$1x10^{-10}$	
G	PbBi		$<1x10^{-11}$	R
H	PbBi		$<1x10^{-11}$	$7x10^{-9}$

Influence of Ba Additions on the Superconducting Properties of Bi-2212

Trociewitz, U.P., NHMFL/RWTH Aachen Univ. of Technology
Sastry, P.V.P.S.S., NHMFL
Sahm, P.R., RWTH Aachen Univ. of Technology
Schwartz, J., NHMFL/FAMU-FSU College of Engineering

Among all high temperature superconductors, Bi-2212 is considered the most suitable material for applications as insert coils for high field magnets. Weak flux pinning, however, imposes a limitation on the application of Bi-2212. We are investigating the influence of BaO_2 additions on the flux pinning behavior in Bi-2212.

BaO_2 reacts with Bi-2212 forming non-superconducting phases, which are small and homogeneously distributed due to their origin in a chemical reaction process during the partial-melt and resolidification process. These precipitates can act as pinning centers in the Bi-2212. Systematic investigations were conducted on the phase assemblage, and the microstructural characteristics of doped and undoped Bi-2212. BaO_2 content and heat treatment process were optimized. Extensive magnetization and transport measurements were carried out. Significant enhancement in magnetization and high field transport properties was achieved in optimally doped tapes (Figure 1).

It was found that BaO_2 reacts with the Bi-2212 to form second phases. It did not enter the lattice of Bi-2212, and therefore did not alter the superconducting phase. No evidence for agglomeration of the formed second phases was found, and the size of the precipitates was smaller than the resolution of the Environmental Scanning Electron Microscope (≥ 200 *nm*). XRD analysis revealed that the second phases that

formed consisted of $BaBiO_3$ related phases. Diffusion couple experiments revealed enhanced growth of the Bi-2212 phase in the direction of the concentration gradient of Ba in the precursor material. Higher amounts of BaO_2 additions, however, cause random growth of Bi-2212 grains, resulting in the formation of high angle grain boundaries, which reduce the transport current (Figure 2). This effect explains the existence of an optimal amount of BaO_2, which was found to be in the range of 2 to 3 wt.%. Further work is in progress to achieve a better distribution of Ba in the Bi-2212 precursor, and to improve the microstructure.

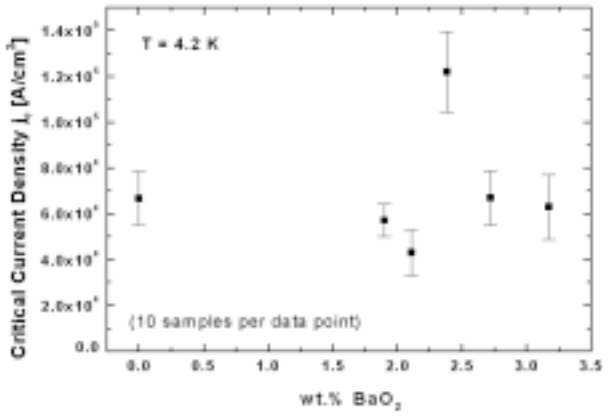

Figure 1. Maximum critical current densities vs. BaO_2 content. The heat treatment process was optimized for each composition.

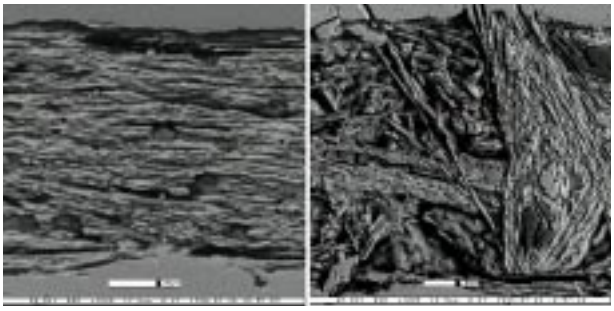

Figure 2. SEM micrographs of a 2.38 wt.% (left) and a 3.17 wt.% (right) BaO_2 doped tapes.

References:

1 Trociewitz, U.P., *et al*, IEEE Trans. Applied Superconductivity, 1998 Applied Superconductivity Conference, to be published.

2 Trociewitz, U.P., *et al.*, Advances in Cryogenic Engineering (Materials), 44, 663 (1998).

Effects of Mechanical Strain on Critical Current Density of Bi-2212

Viouchkov, Y., NHMFL
Weijers, H.W., NHMFL
Hu, Q., NHMFL
Hascicek, Y.S., NHMFL
Schwartz, J., NHMFL/FAMU-FSU College of Engineering

Two types of Bi-2212 tapes supplied by Oxford Superconducting Technology were tested for determination of electro-mechanical properties: composite 19-filament Bi-2212/Ag-AgMg alloy sheathed tape and composite 19-filament Bi-2212/Ag-Ag sheathed tape. Overall, best-obtained performance in terms of critical current (I_c) for Bi-2212/Ag-Ag sheathed tape is 395A, with a cross section of 3.0 x 0.2 mm. The typical critical current density (J_c) performance of AgMg-sheathed conductor is about 20% lower than that of the Ag-sheathed conductor.

Two effective devices for mechanical and transport I_c testing were used to investigate the properties of Bi-2212 tapes. A Linear Tensile Tester was used for stress-strain measurements. A cryogenic chamber was built around the calipers and sample. Figures 1 and 2 shows stress-strain relations for the conductors at room and liquid nitrogen temperatures. A Lorentz Force Device (R) was used to determine I_c vs. stress on ring shaped samples.

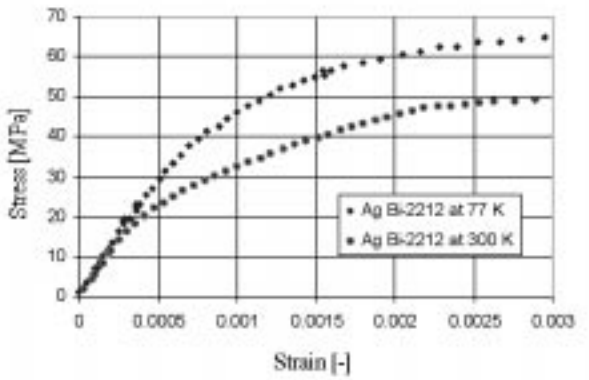

Figure 1. Stress-strain for 2212-Ag conductor.

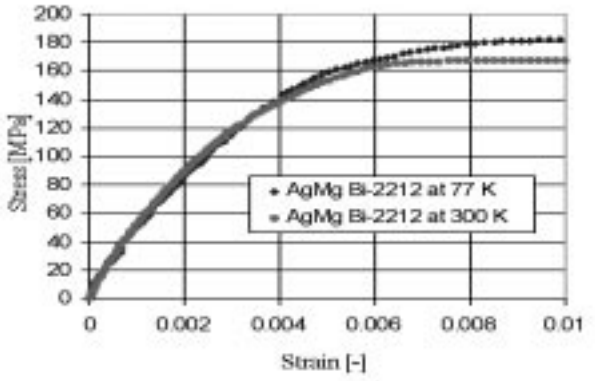

Figure 2. Stress-strain for 2212-AgMg conductor.

Loads were applied at 4.2 K by setting the magnetic field to a fixed value, and ramping the sample's current to a predetermined value. The I_c was measured after the background field was ramped back to 0 T. Figure 3 shows I-V curves used to determine the normalized I_c vs. strain shown in Figure 4.

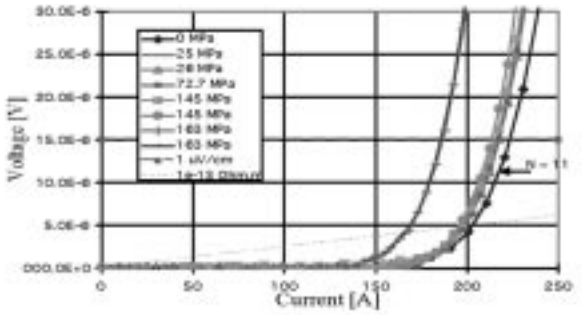

Figure 3. I-V curves after peak stress.

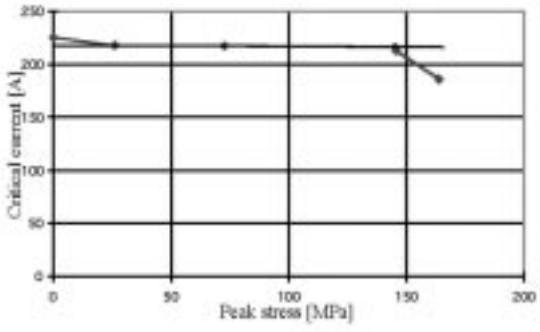

Figure 4. Normalized I_c vs. peak stress.

A small (3%) initial I_c degradation was observed. I_c decreases about 2% per 1% of strain, up to σ=145 MPa, and significant (18%) I_c degradation at σ=164 MPa for Ag-Mg sheathed tape. The Young's modulus of the 2212-Ag conductor was obtained at 77 K (E = 67 ± 2.5 GPa) with the linear tester.

Critical Current Measurements on Large Superconducting Cable Embedded in an Aluminum Stabilizer

Walsh, R.P., NHMFL
Miller, J.R., NHMFL
O'Connor, T.G., Lawrence Livermore National Laboratory

A new detector called *BABAR*, has been designed and constructed at the Stanford Linear Accelerator Center (SLAC). The conductor is composed of a NbTi/Cu superconducting Rutherford cable embedded in a rectangular channel of high purity aluminum (HP-Al). Tests were performed on full-scale conductors using the 13 T split-solenoid test station of NHMFL's Large Magnet Component Test Facility (LMCTF) and the laboratory's main DC power supply. The 4.2 K tests are performed with a constant background field (ranging from 11 T to 7 T), while the test sample current is ramped monotonically, and sample voltage is recorded. The results verify superconductor performance including both critical current and index, under simulated operating conditions. The typical voltage versus current trace at various applied background fields (Figure 1) show the superconductor to resistive transition. The appropriate field (B_t), however, to be considered for a high-current conductor is the worst-case combination of applied field (B_a) and maximum self field (B_s).

In the case of conductors with a large fraction of high-conductivity stabilizer shunting the superconductor, the transfer of a portion of the total current to the stabilizer also modifies the trace. Figure 2 shows the excellent agreement between the test data of the full-scale conductor at 8 T, and the curve generated by the predictive equation for the full-scale conductor. The good agreement between measured and predicted data is observed for all the tests, establishing

confidence that the effects of the HP-Al and self-field have been quantified. Analysis of the data demonstrates that conductor performance is consistent with our understanding, and the properties of a HP-Al stabilized conductor are predictable with a high degree of certainty.

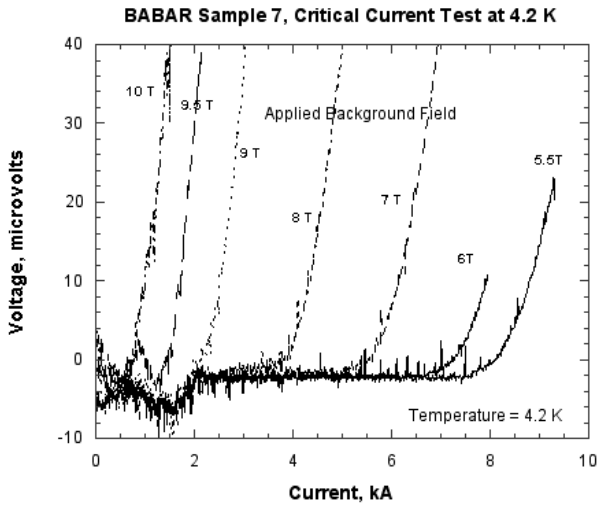

Figure 1. I vs. V data at various applied fields.

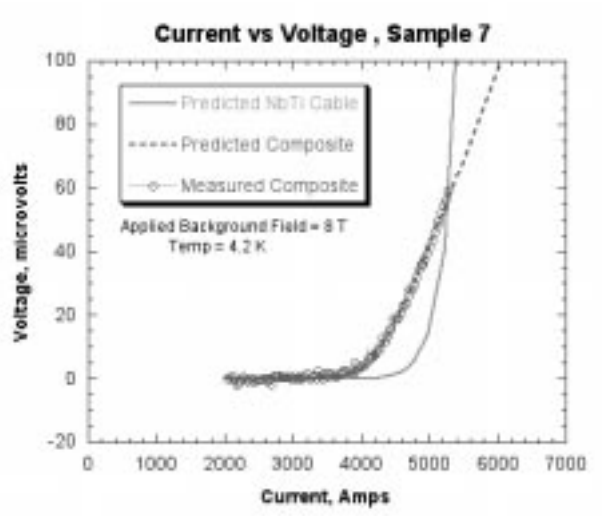

Figure 2. Comparison of measured and predicted data.

The authors would like to thank J. Kenney of NHMFL for his technical expertise in sample preparation, and G. Wendt for his assistance with the tests.

References:

1 GANDALF computer program, Dependence of NbTi critical-current on field and temperature, Cryosoft, 5, rue de la Belette, F-01710 THOIRY, France.

2 Walsh, R.P., *et al*., Proc. IEEE Trans. Appl. Superconductivity, Sept 14-18, 1998, Palm Desert, CA.